SPATIOTEMPORAL ANALYSIS OF AIR POLLUTION BY NO_2 IN URBAN AND RURAL AREAS OF BRAZIL USING GOOGLE EARTH ENGINE AND R

Orlando Eduardo Chipura
Federal University of Lavras, Agricultural Engineering Department, Campus, ZIP Code 307203-202, Lavras, MG, Brazil
Corresponding author: o.chipura@gmail.com

Marcelo de Carvalho Alves
Federal University of Lavras, Agricultural Engineering Department, Campus, ZIP Code 307203-202, Lavras, MG, Brazil

Flávio Vanoni de Carvalho Júnior
Federal University of Lavras, Agricultural Engineering Department, Campus, ZIP Code 307203-202, Lavras, MG, Brazil

Fortunato Silva de Menezes
Federal University of Lavras, Physics Department, Campus, ZIP Code 307203-202, Lavras, MG, Brazil

Bruno de Oliveira Schneider
Federal University of Lavras, Department of Computer Science, Campus, ZIP Code 307203-202, Lavras, MG, Brazil

Abstract: Remote sensing has notably advanced in terms of the information that can be extracted from generated products. The combined use of different sensor systems proves effective in detecting environmental changes and reducing uncertainties about where significant atmospheric pollutant emissions occur. This study aimed to analyze the spatiotemporal variation of atmospheric pollution by NO_2 in urban and rural areas of the states of São Paulo, Rio de Janeiro, and Minas Gerais, Brazil, from September 2023 to September 2024. Tropospheric NO_2 data were collected using the TROPOMI sensor on the Sentinel-5P satellite. The results indicated that urban areas exhibited the highest average levels of atmospheric NO_2 pollution. In the metropolitan region of São Paulo, the average atmospheric NO_2 concentration was 1.90E-04 mol.m^{-2}, followed by the metropolitan region of Rio de Janeiro at 1.10E-04 mol.m^{-2} and the metropolitan region of Belo Horizonte at 0.83E-04 mol.m^{-2}. In rural areas—specifically agricultural and pasture regions—the highest daily average of atmospheric NO_2 pollution was recorded in São Paulo at 1.50E-04 mol.m^{-2}, followed by Rio de Janeiro at 0.94E-04 mol.m^{-2} and Belo Horizonte at 0.66E-04 mol.m^{-2}. From June to August 2024, elevated levels of NO_2 air pollution were observed. This study concludes that metropolitan regions have higher levels of NO_2 pollution compared to rural areas in all three states of Brazil. The burning of fossil fuels in industries, emissions from motor vehicles, and urban waste are likely contributing factors to the higher pollution levels in metropolitan areas compared to rural regions.

Keywords: Remote sensing, Sentinel-5P, time series, fossil fuels, agricultural and pasture areas.

Received: December 3, 2024 - Accepted: January 29, 2025

INTRODUCTION

Air pollution is one of the most critical environmental issues facing both developed and developing countries today (VÎRGHILEANU et al., 2020). High concentrations of nitrogen dioxide (NO_2) and other pollutants result from anthropogenic activities, leading to harmful effects on public health and the environment. These pollutants can cause respiratory and pulmonary problems, trigger allergies, and contribute to the formation of photochemical smog and acid rain (KURIYAMA; MOREIRA; SILVA, 1997; SOUZA; AZEVEDO; DELLA JUSTINA, 2021; VALADÃO et al., 2022; HALDER et al., 2023). Furthermore, they play a role in increasing tropospheric ozone levels while decreasing its concentration in the stratosphere, thereby affecting the Earth's surface warming (KURIYAMA; MOREIRA; SILVA, 1997).

The continued reliance on fossil fuels in urban, agricultural, and pasture areas both globally and in Brazil has led to a differentiated rise in atmospheric (NO_2) levels. Agricultural activities can also contribute to air and soil pollution (ABBASI et al., 2014).

According to various studies, including those by Bechle, Millet, and Marshall (2013), Vîrghileanu et al. (2020), Eduarda Gomes de Souza et al. (2022) and Valadão et al. (2022), NO_2 is a key component of urban air pollution, primarily generated by human actions such as the burning of fossil fuels in land, sea, and air transport. Eduarda Gomes de Souza et al. (2022) note that NO_2 can also be produced naturally, for instance, through lightning strikes. Nitrogen oxides, including nitric oxide NO and nitrogen dioxide (NO_2), are commonly measured using remote sensing technologies such as Sentinel-5P (BECHLE; MILLET; MARSHALL, 2013; SOUZA, E. G. d. et al., 2022; VALADÃO et al., 2022). This highlights the importance of monitoring NO_2 levels in both urban and rural areas, which has been demonstrated in multiple studies, predominantly focused on cities. It has been found that NO_2 has greater toxicity compared to other nitrogen oxides and can significantly aggravate respiratory and other airborne diseases (KURIYAMA; MOREIRA; SILVA, 1997; SOUZA, E. G. d. et al., 2022). NO_2 is capable of damaging the lungs directly through its oxidising properties or indirectly by increasing susceptibility to respiratory infections (KURIYAMA; MOREIRA; SILVA, 1997).

Satellite imagery plays a crucial role in detecting air quality changes and identifying various pollutants in the stratosphere and troposphere. Google Earth Engine (GEE), launched by Google in 2010, offers a platform for storing and processing Earth observation data, making it easier to access satellite data alongside other information through cloud computing (FAISAL et al., 2021; SHAMI et al., 2022; KAZEMI GARAJEH et al., 2023; HALDER et al., 2023; TABUNSCHIK; GORBUNOV; GORBUNOVA, 2023). This technology enables the analysis and processing of large-scale geospatial data (TABUNSCHIK; GORBUNOV; GORBUNOVA, 2023), particularly beneficial for remote sensing science (AZEVEDO; CANDEIAS; TAVARES JÚNIOR, 2021). GEE is vital for mapping and monitoring pollution sources, facilitating local actions to combat air quality issues, which are particularly pressing in developing countries (HALDER et al., 2023).

The European Space Agency's Sentinel-5P satellite, launched on October 13, 2017, is part of the Copernicus program aimed at globally monitoring air quality, climate, and the ozone layer (FAISAL et al., 2021; LEE; LIU; CHATFIELD, 2023). Studies by Azevedo, Candeias, and Tavares Júnior (2021) and Valadão et al. (2022) indicate that data from the Sentinel-5 satellite represents a viable option for air quality monitoring due to the capabilities of the Tropospheric Monitoring Instrument (TROPOMI) sensor, which can perform atmospheric measurements with good spatiotemporal resolution. Moreover, according to Safieddine et al. (2013), satellite-based measurement of tropospheric NO_2 has proven efficient, providing extensive regional and global information.

The TROPOMI sensor provides daily data on air pollution levels, specifically nitrogen dioxide (NO_2) (KAZEMI GARAJEH et al., 2023), measured in mol.m^{-2} (LEE; LIU; CHATFIELD, 2023). This sensor finds application in the field of remote sensing, where it evaluates the concentrations of various polluting gases (VALADÃO et al., 2022; CAKMAK; YILMAZ; BALIK SANLI, 2023).

Currently, there are ongoing discussions to compare NO_2 pollution levels in urban and rural areas of Brazil, particularly due to the growth of agribusiness. According to Lee, Liu, and Chatfield (2023), urban areas are the largest sources of NO_2 emissions when compared to rural regions. This observation holds true for the states of São Paulo, Rio de Janeiro, and Minas Gerais.

The purpose of this article is to analyze and compare the spatiotemporal variation of atmospheric pollution by NO_2 in both urban and rural areas of Brazil.

MATERIAL AND METHODS

Study Area

The study area included three metropolitan and rural regions in Brazil, specifically in the states of São Paulo, Minas Gerais, and Rio de Janeiro. These regions are considered potential sources of pollutant emissions, as shown in the Figure 1, highlighting the urban centers of the states mentioned. The data was collected from initial filtering points located in the metropolitan region of São Paulo; Rio de Janeiro and Belo Horizonte. The rural areas were chosen because they represent the largest coffee production regions in 2023, which may be the reason for the greater amounts of nitrogen fertilizer management, according to IBGE data.

Software and Data Processing Methods

The tools used in this study include Google Earth Engine and RStudio version 4.3.3. The analyses in R were performed using the packages listed in Table 1.

Data Types and Sources

Veefkind et al. (2012), Vîrghileanu et al. (2020), Valadão et al. (2022) and Lee, Liu, and Chatfield (2023) they describe the TROPOMI sensor is a spectrometer that operates in multiple bands: ultraviolet (UV), visible (VIS - 270 to 500 nm), near-infrared (NIR - 675 to 775 nm), and shortwave infrared (SWIR - 2305 to 2385 nm). The sensor captures images using electronic scanning (pushbroom) and has a spatial resolution of 7 km at the sub-satellite point. The width of the imaged swath is 2600 km, and the pixel size is 7 x 3.5 km^2 near nadir for nearly all spectral bands.

Data Collection and Processing

For this research, nitrogen dioxide NO_2 and image data were collected from the European Space Agency (ESA), available through a database integrated with Google Earth Engine (GEE). Data were gathered for monthly periods from September 2023 to September 2024. According Kazemi Garajeh et al. (2023), Google Earth Engine provides researchers with rapid access to over thirty years of publicly available data archives, including historical images and scientific datasets for remote sensing applications.

Data processing and analysis were conducted using both Google Earth Engine (GEE) and R environments, with coding performed in JavaScript and R, respectively, as illustrated in the flowchart in Figure 2. Monthly and annual averages of NO_2 were calculated using data from the Sentinel-5P TROPOspheric Monitoring Instrument (TROPOMI) accessed through the GEE platform.

The average concentration of NO_2 was calculated for six points that identify the data collection areas and the corresponding pixels: 1. São Paulo metropolitan region, 2. Rio de Janeiro, 3. Belo Horizonte and 4. Fazenda Monte Alegre, 5. Fazenda Vargem Alegre and 6. Fazenda Castelhana Agrocafé, 2029122, 1789269, 679555, 802421, 1045963, 274397, respectively. The monthly and annual averages of NO_2 were then calculated for the historical series, corresponding to the urban and rural agricultural areas. The "Sentinel-5P L3" collection was used to estimate the concentration of NO_2 using - ee.ImageCollection (COPERNICUS/S5P/OFFL/L3_NO$_2$). The daily data collected was then stored in CSV format, while the images were saved in TIFF format on Google Drive.

Using Google Earth Engine, JavaScript language, the atmospheric concentration map of NO_2 was created. Four pollution parameters from Sentinel-5 satellite images were analyzed. The daily data collected by the satellite was filtered to remove images covered by clouds and to calculate the average for the year under analysis. The code in Figure 3 was used to process the previously georeferenced images in the Google Earth Engine.

Based on the images and the CSV file from GEE, we generated geospatial variation maps, graphs, and descriptive statistics tables concerning the temporal variation of NO_2. This was achieved using R packages such as `terra`, `sf`, `geobr`, `ggplot2`, `grid`, `dplyr`, `readr`, and `knitr`, within RStudio 4.3.3 software, which is free and open-source (SOUZA, E. G. d. et al., 2022). The code in Figure 4 was used to create

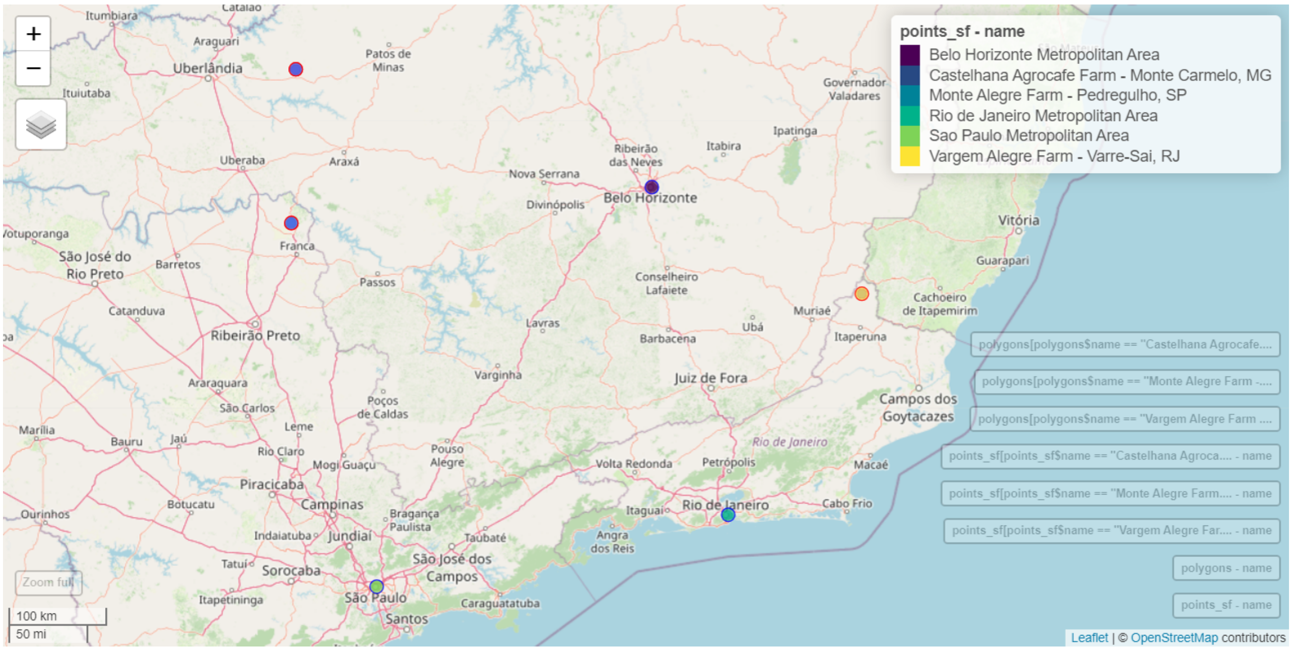

Figure 1: Location of the study area, highlighting the metropolitan and rural regions of the states of São Paulo, Rio de Janeiro, and Minas Gerais, Brazil, from September 2023 to September 2024. Image collected from Mapview in R.

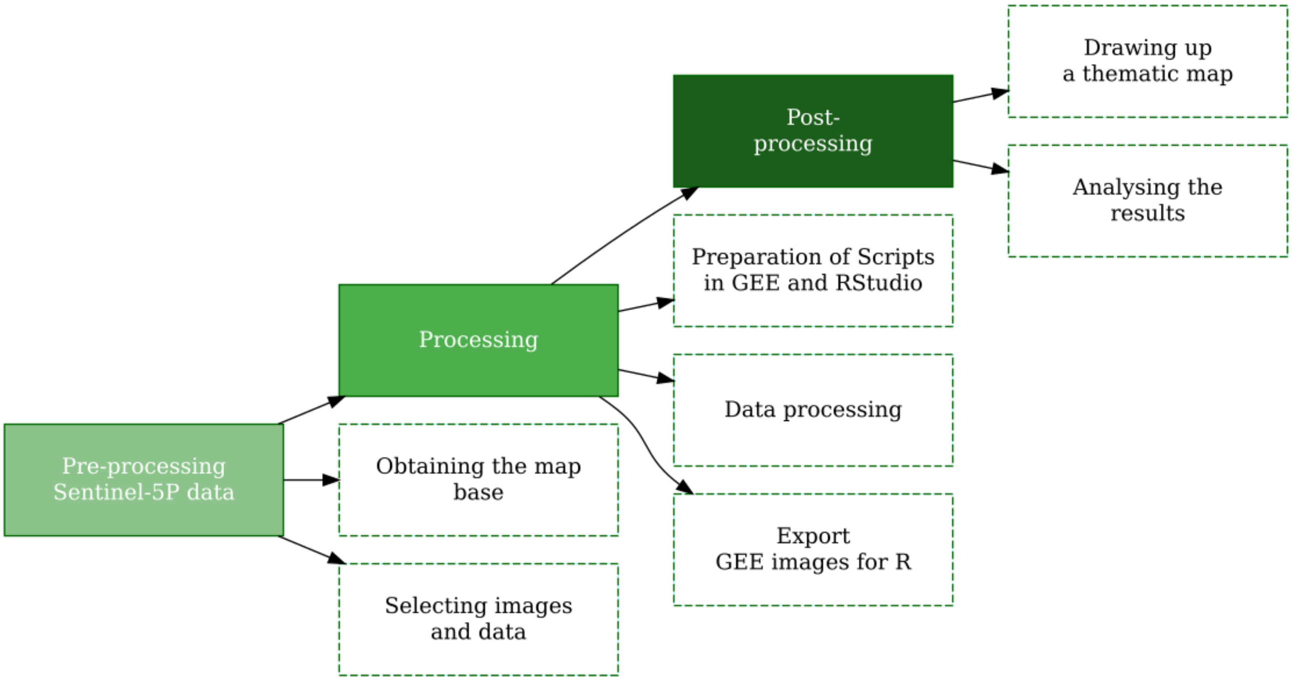

Figure 2: Methodological flowchart for the analysis and comparison of air pollution in the metropolitan and rural regions of São Paulo, Rio de Janeiro, and Belo Horizonte, Brazil, from September 2023 to September 2024.

Table 1: R packages utilized in the research for analyzing atmospheric pollution levels of NO_2.

Package	Description	Reference
ggplot2	It was used in the implementation of graph grammar and for mapping survey data.	Wickham (2016)
sf	It was used for geometric operations and 'PROJ' for projection conversions and datum transformations.	Pebesma (2018)
readr	It was used to read rectangular NO_2 data in csv format.	Wickham, Hester, and Bryan (2024)
terra	It was used for spatial prediction with satellite remote sensing data. Processing of very large files was supported.	Hijmans et al. (2023)
geobr	It is configured as an accessible and practical solution for accessing official spatial data sets from the Brazilian territory.	Menezes (2023)
knitr	This package provides a general purpose tool for dynamically generating reports and displaying formatted tables in R.	Xie (2015)
dplyr	It was used for data manipulation and working with data frame type objects.	Wickham (2011)

```
// Define the areas of interest in a single geometry
var regioesMetropolitanas = ee.Geometry.MultiPolygon([
  ee.Geometry.Rectangle([-49.0, -25.0, -45.5, -22.0]), // SP
  ee.Geometry.Rectangle([-45.5, -23.9, -41.5, -20.8]), // RJ
  ee.Geometry.Rectangle([-49.0, -22.2, -41.5, -18.1]) // BH ])

// Add points for the coffee units
var pontosCafeeiros = ee.FeatureCollection([
ee.Feature(ee.Geometry.Point([-41.883, -20.902]), {name: 'Vargem_Alegre_Farm_RJ'),
ee.Feature(ee.Geometry.Point([-47.457, -20.253]), {name: 'Monte_Alegre_Farm_SP'),
ee.Feature(ee.Geometry.Point([-47.421, -18.835]), {name: 'Castelhana_Agrocafe_MG')
]);

// Import Sentinel-5P data for nitrogen dioxide \text{NO$_{2}$} and filter
for the period of interest
var s5p_no2 = ee.ImageCollection('COPERNICUS/S5P/NRTI/L3_NO2')
.select('\text{NO$_{2}$}_column_number_density')
.filterDate('2023-09-01', '2024-09-30');

// Calculate the average \text{NO$_{2}$} for the unified region
var mediaNO2Regioes = s5p_no2.mean().clip(metropolitan regions);

// Export the average \text{NO$_{2}$} of the unified region to Google Drive
Export.image.toDrive({
  image: mediaNO2Regions,
  description: 'Media_\text{NO$_{2}$}_Metropolitan_and_Rural_Regions_2023_2024',
  folder: 'EarthEngine',
  fileNamePrefix: '\text{NO$_{2}$}_Metropolitan_and_Rural_Regions',
  region: metropolitan regions,
  scale: 500,
  maxPixels: 1e13,
  crs: 'EPSG:4326' })
```

Figure 3: Example javascript code used to define area of interest, import and filter Sentinel-5P data, calculate average and import GEE TIFF file, from September 2023 to September 2024.

the map of the concentration of NO_2 in urban and rural areas using the R language.

GEE also provided access to a free geospatial database, facilitating the manipulation of large-scale datasets and long time series (VALADÃO et al., 2022; KAZEMI GARAJEH et al., 2023); this data was used with the R language for descriptive statistical analysis and the creation of graphs of the temporal variation of pollution by NO_2 in the urban and rural regions..

RESULTS AND DISCUSSION

This section presents the results of analyses regarding the spatial and temporal variation of atmospheric pollution by NO_2 in the metropolitan and rural regions of São Paulo, Rio de Janeiro, and Minas Gerais.

Spatial Variation of Atmospheric Pollution by NO_2 in Metropolitan and Rural Regions

The annual averages for ambient concentrations of NO_2 measured by the TROPOMI sensor on Sentinel-5P for the metropolitan regions of São Paulo, Rio de Janeiro, and Belo Horizonte were 1.90E-04, 1.10E-04, and 0.83E-04 mol.m^{-2}, respectively. For the rural areas in the states of São Paulo, Rio de Janeiro, and Minas Gerais, the averages were 1.50E-04, 0.94E-04, and 0.66E-04 mol.m^{-2}, respectively, as shown in Table 2 and studies by Miranda et al. (2012). .

The results presented in Table 2 illustrate the variation in atmospheric NO_2 concentration between urban and rural regions in São Paulo, Rio de Janeiro, and Minas Gerais. In comparing atmospheric NO_2 concentration levels across historical time series, the metropolitan region of São Paulo exhibited the greatest variation from the series average, reported at 1.90E-04 mol.m^{-2}. This was followed by the metropolitan regions of Rio de Janeiro and Belo Horizonte. Analyzing the data, we observed a difference of 0.80E-04 mol.m^{-2} in NO_2 concentration between the metropolitan regions of São Paulo and Rio de Janeiro. A more substantial difference was apparent when comparing the concentration levels of metropolitan São Paulo and Belo Horizonte, with a corresponding difference of 1.07E-04 mol.m^{-2}. The disparity between Rio de Janeiro and Belo Horizonte was recorded as 0.27E-04 mol.m^{-2}. Consequently, the metropolitan region of São Paulo demonstrated the highest concentration of atmospheric NO_2.

Based on the study by Eduarda Gomes de Souza et al. (2022), the states of São Paulo (SP) and Rio de Janeiro (RJ) have experienced high levels of tropospheric NO_2 concentration. This is largely due to their large urban centers, high industrialization, dense populations, and heavy vehicle traffic, which are the main sources of NO_2 emissions.

The results indicate that the concentration of NO_2 in the metropolitan regions of the analyzed states is higher than in the surrounding rural areas. The data show that the atmospheric NO_2 concentration is relatively low in rural regions. The annual average concentrations reveal that the rural area of São Paulo had the highest NO_2 levels, followed by the rural regions of Rio de Janeiro and Minas Gerais, with values of 1.50E-04, 0.94E-04, and 0.66E-04 mol.m^{-2}, respectively. Thus, the difference between the rural areas of São Paulo and Rio de Janeiro is 0.56E-04 mol.m^{-2}, the difference between São Paulo and Minas Gerais is 0.84E-04 mol.m^{-2}, and the difference between Rio de Janeiro and Minas Gerais is 0.28E-04 mol.m^{-2}. Overall, these comparisons highlight that the metropolitan regions have the highest concentrations of NO_2.

In contrast, Bechle, Millet, and Marshall (2013), Vîrghileanu et al. (2020), Eduarda Gomes de Souza et al. (2022) and Valadão et al. (2022) the difference in NO_2 concentration between rural São Paulo and Rio de Janeiro is 1.20E-04 mol.m^{-2}, while the difference between Rio de Janeiro and Minas Gerais is 1.38E-04 mol.m^{-2}. Therefore, the difference in NO_2 concentration between rural areas of São Paulo and Minas Gerais is 1.38E-04 mol.m^{-2}. According to Eduarda Gomes de Souza et al. (2022), the high levels of tropospheric NO_2 concentration in São Paulo and Rio de Janeiro result from their extensive urban centers, high levels of industrialization, large populations, and significant vehicle traffic, which are the primary sources of NO_2 emissions.

```
#The geobr, terra, ggplot2, sf, scales packages were released using the library.
#NO2_Rural_Metropolitan_Regions.tif imported from Google Drive was considered
prepared in GEE

# Set the path to the image downloaded from Google Drive
image_path <- "C:/Users/OneDrive/Documentos/NO2_Rural_Metropolitan_Regions.tif"

#Load the raster file with the terra library
pollution_no2 <- rast(image_path)

# Convert the raster to a data frame for use in ggplot2
pollution_df <- as.data.frame(pollution_no2, xy = TRUE)

# Load the map of Brazilian states and filter only SP, RJ and MG
states <- read_state()
highlight_states <- states[states$abbrev_state %in% c("RJ", "MG", "SP"),]

# Define coordinates for cities and farms
locations <- data.frame(
  lon = c(-46.6333, -43.1729, -43.9352, -47.4211, -47.4730, -41.8708),
  lat = c(-23.5505, -22.9068, -19.9245, -18.8357, -20.2534, -20.9047),
  nome = c(
    "SP_metropolitan", "RJ_metropolitan", "BH_metropolitan",
    "Castelhana_Agrocafe_Farm",  "Monte_Alegre_Farm",
    "Vargem_Alegre_Farm"))

# Converter os pontos para um objeto sf
locations_sf <- st_as_sf(locations, coords = c("lon", "lat"), crs = 4326)

#Plot the pollution map and overlay the points of the cities and farms using the
ggplot2 package
```

Figure 4: Example of R computer language code used to process the GEE TIFF file to map NO_2 air pollution in the area of interest, from September 2023 to September 2024.

Table 2: Descriptive statistics of the concentration of NO_2 in urban and rural regions of the states of São Paulo (SP), Rio de Janeiro (RJ), and Minas Gerais (MG), Brazil, from September 2023 to September 2024.

Region	Data	NO_2 concentration (xE-04)				
		Minimum	Maximum	Average	Standard Deviation	Median
Urban BH	421	0.21	2.30	0.83	0.31	0.78
Urban RJ	408	0.00	2.90	1.10	0.45	0.99
Urban SP	400	0.43	8.10	1.90	1.10	1.60
Rural MG	426	0.056	2.30	0.66	0.20	0.63
Rural RJ	403	0.30	3.50	0.94	0.35	0.88
Rural SP	410	0.30	6.30	1.50	0.80	1.30

According to Hulin, Caillaud, and Annesi-Maesano (2010), urban areas are generally more polluted than rural ones, with pollutant concentrations that can be up to twice as high. NO_2 is emitted into the atmosphere primarily due to human activities, especially fossil fuel combustion and biomass burning (ZHAO et al., 2020; CAKMAK; YILMAZ; BALIK SANLI, 2023; KAZEMI GARAJEH et al., 2023). Natural processes such as forest fires, lightning, and microbiological activity in the soil (CAKMAK; YILMAZ; BALIK SANLI, 2023), along with emissions from fertilizer industries, industrial furnaces, boilers, and agricultural activities (CAMPOS et al., 2006), contribute to the pollution levels observed in the metropolitan regions of São Paulo, Rio de Janeiro, and Belo Horizonte.

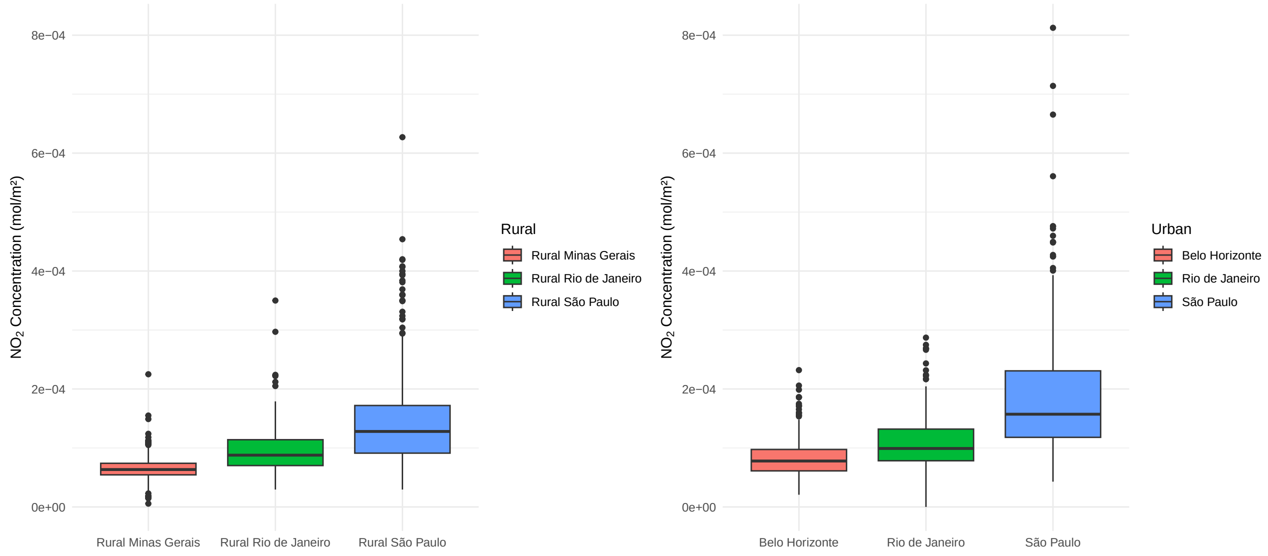

Figure 5: Boxplot of descriptive statistics of NO_2 values at times of maximum and minimum concentrations in the metropolitan regions of São Paulo, Rio de Janeiro, and Belo Horizonte, Brazil, from September 2023 to September 2024.

According to Safieddine et al. (2013), nitrogen dioxide NO_2 air pollution in rural areas primarily reflects local sources. The authors note that rural NO_2 levels are generally lower than those found in urban areas, except in cities like Beijing, where significant local emissions and strong winds may contribute to higher levels.

Bechle, Millet, and Marshall (2013), Vîrghileanu et al. (2020), Eduarda Gomes de Souza et al. (2022) and Valadão et al. (2022) emphasize that NO_2 is a significant component of urban air pollution, which likely explains its reduced presence in rural areas.

A study conducted in California by Lee, Liu, and Chatfield (2023) revealed that the average NO_2 concentration in urban areas was 2.1 times higher than in rural areas, based on a spatial map of estimated NO_2 concentrations at a 500 meter resolution. This finding aligns with our observations in the current research. The authors also point out that a combination of mobile NO_2 emissions and the uneven distribution of road networks, which varies by vehicle types and traffic volumes, contributes to substantial spatial variation in NO_2 levels. Additionally, the relatively short atmospheric lifetime of NO_2 due to chemical reactions results in higher concentrations near emission sources, with levels sharply decreasing as one moves away from these sources, such as highways.

This study also showed that the average concentration of NO_2 is relatively higher in the rural areas of São Paulo (1.50E-04 mol.m^{-2}) compared to the metropolitan regions of Rio de Janeiro (1.10E-04 mol.m^{-2}) and Belo Horizonte (0.83E-04 mol.m^{-2}). The variation in the concentration of NO_2 observed may depend on meteorological parameters such as wind and temperature. Contreras and Ferri (2016) and Vîrghileanu et al. (2020) state that wind is the most important meteorological parameter, which can disperse pollutants in just a few minutes, depending on the wind speed, and can transport them far from the emission sources, which may be the reason for the high concentration in the rural areas of the state of São Paulo compared to the urban area (metropolitan region) of Rio de Janeiro and Belo Horizonte. Temperature is another climatic parameter that can be taken into account, especially in situations of thermal inversions, when the layer of warmer air above the colder surface air acts as a barrier, preventing the rise of the latter and favoring increased contamination of the ambient air Su et al. (2008) and Vîrghileanu et al. (2020).

Figure 6, filtered and processed in Google Earth Engine (GEE), illustrates the spatial variation of atmospheric nitrogen dioxide NO_2 concentration in metropolitan regions in greater detail compared to rural areas. Figure 7, processed in R using the TIFF image generated and imported from GEE, provides a clearer comparison of spatial variations in atmospheric pollution from NO_2 across the three states being analyzed, with particular emphasis on metropolitan regions.

Temporal Variation of Atmospheric Pollution by NO_2 in Metropolitan and Rural Regions

Table 3 presents the results of the monthly averages of NO_2 concentration over the historical series, indicating monthly fluctuations. The highest average concentration of NO_2 was recorded in July, reaching 3.0E-04 mol.m^{-2} in the metropolitan region of São Paulo. The metropolitan region of Rio de Janeiro showed an average monthly concentration of 1.40E-04 mol.m^{-2} during May and June, while the metropolitan region of Belo Horizonte recorded an average of 1.0E-04 mol.m^{-2}. The difference in NO_2 concentration between São Paulo and Rio de Janeiro is 1.60E-04 mol.m^{-2}, while the difference between Rio de Janeiro and Belo Horizonte is 0.40E-04 mol.m^{-2}. Additionally, a difference of 2.0E-04 mol.m^{-2} was observed between the metropolitan regions of São Paulo and Belo Horizonte.

The average monthly concentrations of nitrogen dioxide (NO_2) show similar patterns in rural areas. The highest average concentration was recorded in rural São Paulo at 2.30E-04 mol·m^{-2} during July. This was followed by the rural region of Rio de Janeiro, which had an average concentration of 1.10E-04 mol·m^{-2} observed in June, August, and September. Finally, rural Minas Gerais showed an average concentration of approximately 0.92E-04 mol·m^{-2} in September.

The difference in NO_2 concentration between rural São Paulo and Rio de Janeiro is 1.20E-04 mol·m^{-2}, while the difference between Rio de Janeiro and Minas Gerais is 1.38E-04 mol·m^{-2}. Consequently, the difference in NO_2 concentration between rural São Paulo and Minas Gerais is also 1.38E-04 mol·m^{-2}. Amaury de Souza et al. (2022), states that the maximum concentration of NO_2 is observed in the dry season, from July to September, while the minimum value is recorded in the rainy season, from October to March. This fact was also observed in this study, as shown in Table 3. Therefore, from September to March, there was a reduction in the concentration of NO_2, probably due to the occurrence of rainfall, which starts at the beginning of October and lasts until the beginning of March.

Therefore, Amaury de Souza et al. (2022) state that fires are associated with the clearing of areas for agriculture and contribute to increasing concentrations of NO_2, a practice associated with the dry season, which may explain the concentration levels of NO_2 in rural areas of the states of São Paulo, Rio de Janeiro and Minas Gerais. For Duncan et al. (2003) and Ghude et al. (2009) they state that large biomass burning events can be seen mainly during the period from June to September and during the dry season in South America, the region where Brazil is located, and in Australia. Sheel et al. (2010) state that the contribution of biomass burning to total NO_2 emissions is very small, and therefore this fact may be the most appropriate explanation for the low levels of NO_2 air pollution in rural areas compared to urban areas, that is, the metropolitan regions of São Paulo, Rio de Janeiro and Belo Horizonte, which are more industrialized, with higher levels of vehicle traffic and the burning of fossil fuels, especially during the dry season.

However, Rana et al. (2018) state that changes in meteorological parameters (e.g. air temperature, relative humidity, wind speed, precipitation, solar radiation and cloud fraction), atmospheric chemistry and surface emissions largely determine seasonally dependent NO_2 concentrations, affecting the abundance of NO_2 through removal, transformation and transport processes. Sheel et al. (2010) state that during the winter, as temperatures are low, this leads to a decrease in the rate of loss of NO_2 through photolysis. In addition, the low precipitation during the winter makes fewer OH radicals available, again increasing the useful life of

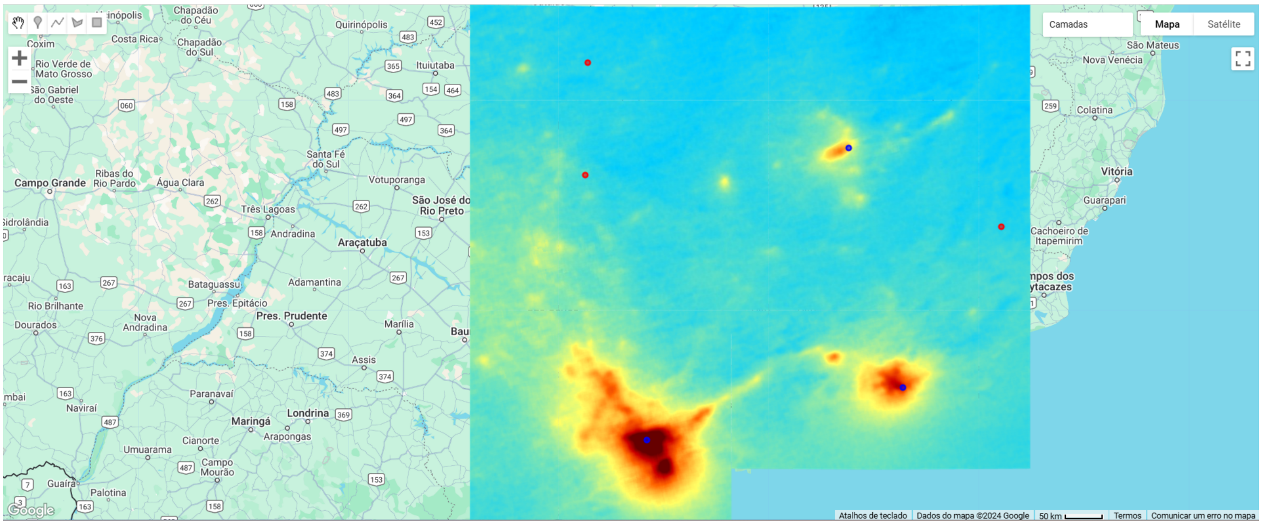

Figure 6: Spatial variation of NO_2 pollution in the states of São Paulo, Rio de Janeiro and Minas Gerais, blue dot (metropolitan region) and red dot (rural region), Brazil, from September 2023 to September 2024. Image collected from GEE.

NO_2. Therefore, Miranda et al. (2012) state that in the states of São Paulo, Rio de Janeiro, Belo Horizonte, winter is characterized by lower temperatures, lower relative humidity and less precipitation, probably resulting in higher concentrations of NO_2 in the dry season and winter.

According to Hulin, Caillaud, and Annesi-Maesano (2010), urban areas are generally considered more polluted than rural ones, with concentrations of NO_2 reaching up to twice as high in cities. NO_2 is released into the atmosphere due to human activities, particularly from fossil fuel combustion and biomass burning (ZHAO et al., 2020; CAKMAK; YILMAZ; BALIK SANLI, 2023; KAZEMI GARAJEH et al., 2023), as well as natural processes such as forest fires, lightning strikes, and microbiological activities in the soil (CAKMAK; YILMAZ; BALIK SANLI, 2023). Other sources of NO_2 include the fertilizer industry, industrial furnaces, boilers, and agricultural activities (CAMPOS et al., 2006). These sources are prevalent in the metropolitan areas of São Paulo, Rio de Janeiro, and Belo Horizonte, potentially contributing to the pollution levels observed in this study.

The monthly variation in NO_2 concentration showed that the metropolitan region of São Paulo had the highest average level, reaching 3.0E-04 mol.m^{-2} in June. Rio de Janeiro followed with an average of 1.40E-04 mol.m^{-2} in both May and June. Belo Horizonte recorded an average of 1.0E-04 mol.m^{-2} in August. In the rural areas, the rural region of São Paulo had the highest atmospheric pollution level, with a concentration of 2.30E-04 mol.m^{-2} in March. This was followed by Rio de Janeiro at 1.20E-04 mol.m^{-2} in April, and Minas Gerais, which recorded 0.84E-04 mol.m^{-2} in May.

Figure 8 illustrates the average monthly variation of air pollution levels, specifically due to nitrogen dioxide (NO_2). The historical data from metropolitan and rural regions indicates a seasonal pattern in air pollution levels. Specifically, during the months of March, April, May, June, and July—the transition from the rainy to the dry season—higher concentrations of NO_2 are observed. In contrast, the months of September, October, November, December, January, February, and August, which encompass the end of the dry season and the entirety of the rainy season, show lower pollution levels.

According to Eduarda Gomes de Souza et al. (2022), major urban centers in the states of São Paulo and Rio de Janeiro exhibit significant variation in NO_2 concentrations. In São Paulo, the extreme high values are attributed to the combustion of fossil fuels stemming from industrial activities, vehicle emissions, and the burning of urban waste, which is not exclusively linked to these sources.

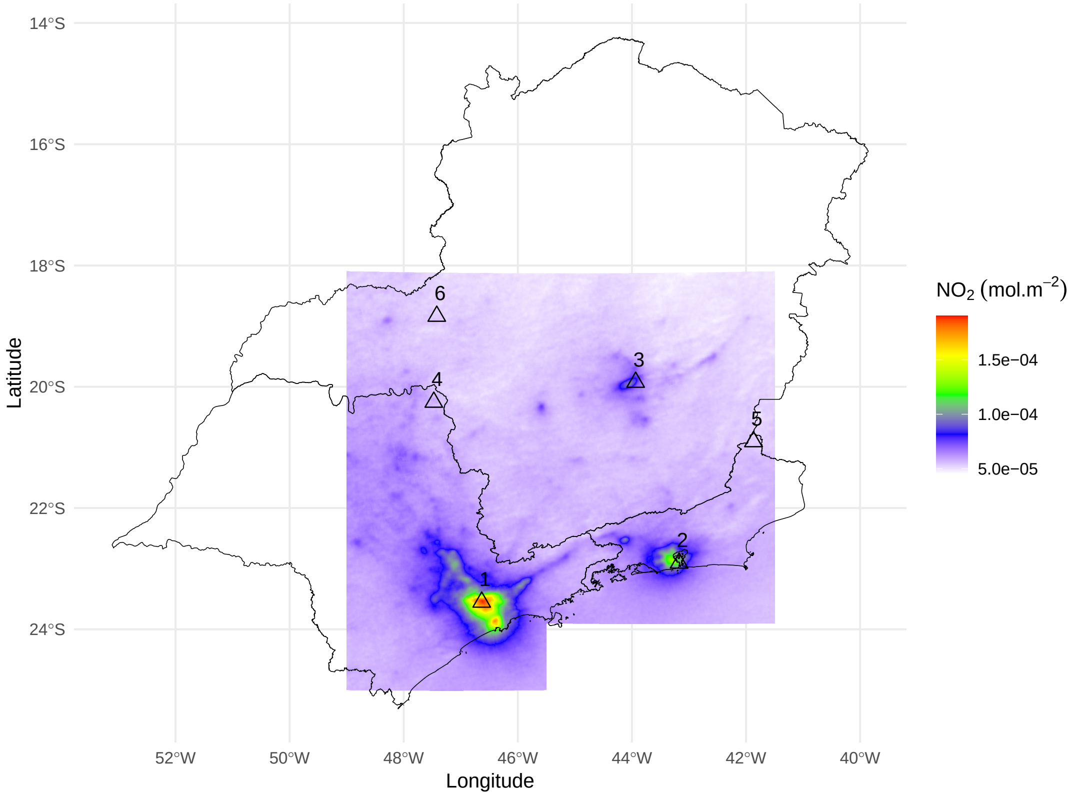

Figure 7: Spatial variation of NO_2 pollution in the states of 1. São Paulo, 2. Rio de Janeiro, 3. Belo Horizonte metropolitan region and 4. Monte Alegre Farm, 5. Vargem Alegre Farm and 6. Castelhana Agrocafé Farm in rural areas, Brazil, from September 2023 to September 2024. Image collected from GEE and processed in R.

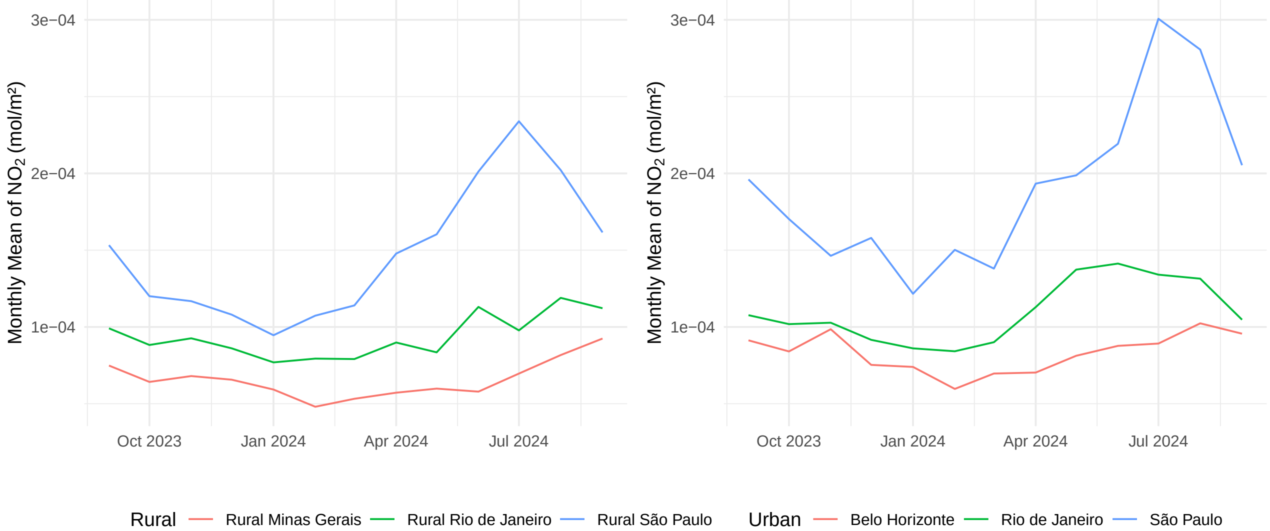

Figure 8: Monthly variation of air pollution by NO_2 in the urban and rural regions of São Paulo, Rio de Janeiro, and Minas Gerais, Brazil, from September 2023 to September 2024.

Table 3: Variation of the monthly average of NO_2 concentration in urban and rural regions of the states of São Paulo (SP), Rio de Janeiro (RJ), and Minas Gerais (MG), Brazil, from September 2023 to September 2024

Region	Set (xE-04)	Out (xE-04)	Nov (xE-04)	Dez (xE-04)	Jan (xE-04)	Fev (xE-04)	Mar (xE-04)	Abr (xE-04)	Mai (xE-04)	Jun (xE-04)	Jul (xE-04)	Ago (xE-04)	Set
Urban BH	0.91	0.84	0.99	0.75	0.74	0.60	0.70	0.70	0.81	0.88	0.89	1.00	0.96
Urban RJ	1.10	1.00	1.00	0.92	0.86	0.84	0.90	1.10	1.40	1.40	1.30	1.30	1.04
Urban SP	2.00	1.70	1.50	1.60	1.20	1.50	1.40	1.90	2.00	2.20	3.0	2.80	2.10
Rural MG	0.75	0.64	0.68	0.66	0.59	0.48	0.53	0.57	0.60	0.58	0.70	0.82	0.92
Rural RJ	0.99	0.88	0.93	0.86	0.77	0.79	0.79	0.90	0.84	1.10	0.98	1.10	1.10
Rural SP	1.50	1.20	1.10	1.10	0.95	1.10	1.10	1.50	1.60	2.0	2.30	2.0	1.60

As noted by Safieddine et al. (2013), air pollution from NO_2 in rural areas typically reflects local sources. The authors found that rural NO_2 levels are generally lower than urban levels, except in exceptional cases like Beijing, where strong winds may disperse pollutants or contribute to significant local emissions.

The trends observed in this study align with the findings reported by Valadão et al. (2022), who highlight a temporal pattern in NO_2 concentrations. They noted that NO_2 density is at its lowest in March and April, while September and October experience unusually high levels, contradicting the expected results. In the metropolitan region of Rio de Janeiro and Belo Horizonte, the lowest concentrations were recorded in February, while January saw the lowest levels in São Paulo. In rural Minas Gerais, reduced monthly variation was also noted in February.

The lowest average NO_2 concentrations in the rural areas of Rio de Janeiro and São Paulo were documented in January. According to Halder et al. (2023), variations in NO_2 levels are indicative of significant anthropogenic activity during this time. The same authors point out that NO_2 is often concentrated in regions where agricultural waste and fossil fuels are burned.

Further supporting these observations, Meng et al. (2010) found that NO_2 peaks during winter and reaches its minimum during summer, a trend also observed in this analysis. As stated by Silva (2023), the Cerrado region's NO_2 concentrations reached notable peaks in August, September, and October due to intense fires that increase NO_2 production. However, in this study, the peak was identified in July at 3.0E-04 mol.m^{-2}, followed by a decrease to 0.90E-04 mol.m^{-2} in September for the metropolitan area. In rural regions, NO_2 concentration decreased from 2.30E-04 mol.m^{-2} in July to 0.70E-04 mol.m^{-2} in September, reflecting the end of the dry season and winter.

The distribution of NO_2 pollution can also be influenced by local meteorological conditions, particularly strong winds that rapidly disperse pollutants and transport them away from sources, as detailed by Julián, ES, and Ferri (2015), Contreras and Ferri (2016) and Vîrghileanu et al. (2020). This factor is crucial in understanding the levels of air pollution from NO_2 across the analyzed regions, which tend to have higher concentrations in winter when wind speeds are lower. Additionally, fossil fuels are utilized in rural areas for cooking purposes (HALDER et al., 2023).

The anthropogenic activities noted in major urban centers, along with the resultant fires in rural areas where agribusiness opens new agricultural and pasture lands, also contribute to NO_2 emissions. The high levels of fertilizer produced by industries are noted by researchers Bechle, Millet, and Marshall (2013), Vîrghileanu et al. (2020), Eduarda Gomes de Souza et al. (2022) and Valadão et al. (2022), emphasizing that NO_2 is a primary component of urban air pollution, largely resulting from human activities and fossil fuel combustion. This pollutant is emitted from land, sea, and air transportation.

Thus, utilizing ground-based NO_2 data is essential for comparing and validating the results obtained.

What can be considered in this analysis are the anthropogenic actions registered in the main urban centers and the consequent fires that occur in rural areas, dependent on agribusiness to open up new agricultural areas and pastures. The high level of fertilizer production by the industry, as defended by researchers Bechle, Millet, and Marshall (2013), Vîrghileanu et al. (2020), Eduarda Gomes de Souza et al. (2022)

and Valadão et al. (2022) NO_2 is one of the main components of urban air pollution and is generated mainly by anthropogenic actions, such as the burning of fossil fuels. In this environment, NO_2 also comes from land, sea and air transportation.

Using ground-based NO_2 data is vital for comparing and validating the results obtained from the TROPOMI sensor data. Lee, Chatfield, and Bell (2018) and Lee, Liu, and Chatfield (2023) argue that while the TROPOMI NO_2 data can illustrate the spatial variation of ambient NO_2 levels, incorporating land-use parameters offers a better explanation for the fine-scale NO_2 variability observed around ground monitoring stations. This integration improves the overall predictive power regarding ambient NO_2 concentrations. The authors highlight that since most NO_2 ground monitoring sites are situated in urban areas, the differing diurnal patterns of NO_2 between urban, suburban, and rural zones can introduce uncertainty in estimating NO_2 concentrations in suburban and rural regions. Thus, utilizing the TROPOMI sensor proves to be an effective way to monitor air quality in large areas, particularly in rural locations where ground monitoring opportunities are limited.

CONCLUSIONS

This study concludes that the metropolitan region of São Paulo experienced higher levels of atmospheric NO_2 pollution, followed by Rio de Janeiro and Belo Horizonte, between September 2023 and September 2024.

In all the states analyzed, rural areas exhibited lower NO_2 levels compared to the metropolitan regions.

Additionally, periods of heavy rain seem to impair the detection of gases, while higher concentrations are typically associated with dry periods, during which fires may impact the regions.

REFERENCES

ABBASI, A. et al. Agricultural pollution: an emerging issue. In: IMPROVEMENT of Crops in the Era of Climatic Changes: Volume 1. [S.l.]: Springer, 2014. P. 347–387. DOI: 10.1007/978-1-4614-8830-9_13.

AZEVEDO, L. d. S.; CANDEIAS, A. L. B.; TAVARES JÚNIOR, J. R. Análise de mudanças na poluição atmosférica e sua relação com o isolamento social em função da pandemia da COVID-19 no Nordeste Brasileiro. **Sociedade & Natureza**, SciELO Brasil, v. 33, e59412, 2021. DOI: 10.14393/SN-v33-2021-59412.

BECHLE, M. J.; MILLET, D. B.; MARSHALL, J. D. Remote sensing of exposure to NO2: Satellite versus ground-based measurement in a large urban area. **Atmospheric Environment**, Elsevier, v. 69, p. 345–353, 2013. DOI: 10.1016/j.atmosenv.2012.11.046.

CAKMAK, N.; YILMAZ, O. S.; BALIK SANLI, F. Spatio-temporal Analysis of Pollutant Gases using Sentinel-5P TROPOMI Data on the Google Earth Engine during the COVID-19 Pandemic in the Marmara Region, Türkiye. **e-Zbornik, elektronički zbornik radova Građevinskog fakulteta**, Sveuči lište u Mostaru, v. 13, n. 25, p. 1–14, 2023. DOI: 10.47960/2232-9080.2023.25.13.1.

CAMPOS, V. P. et al. Monitoramento atmosférico passivo de SO2, NO2 e O3 em áreas urbanas e de influência industrial como prática de química ambiental para alunos de graduação. **Química Nova**, SciELO Brasil, v. 29, p. 872–875, 2006. DOI: 10.1590/S0100-40422006000400042.

CONTRERAS, L.; FERRI, C. Wind-sensitive interpolation of urban air pollution forecasts. **Procedia Computer Science**, Elsevier, v. 80, p. 313–323, 2016. DOI: 10.1016/j.procs.2016.05.343.

DUNCAN, B. N. et al. Interannual and seasonal variability of biomass burning emissions constrained by satellite observations. **Journal of Geophysical Research: Atmospheres**, Wiley Online Library, v. 108, n. D2, ach–1, 2003. DOI: 10.1029/2002JD002378.

FAISAL, M. et al. Spatio-Temporal Analysis of Air Pollutants Changes During The COVID-19 Using Sentinel-5P in Google Earth Engine (Case Study: Java Island). In: IEEE. 2021 IEEE Asia-Pacific Conference on Geoscience, Electronics and Remote Sensing Technology (AGERS). [S.l.: s.n.], 2021. P. 102–108. DOI: 10.1109/AGERS53903.2021.9617331.

GHUDE, S. D. et al. Satellite derived trends in NO2 over the major global hotspot regions during the past decade and their inter-comparison. **Environmental Pollution**, Elsevier, v. 157, n. 6, p. 1873–1878, 2009. DOI: 10.1016/j.envpol.2009.01.013.

HALDER, B. et al. Machine learning-based country-level annual air pollutants exploration using Sentinel-5P and Google Earth Engine. **Scientific Reports**, Nature Publishing Group UK London, v. 13, n. 1, p. 7968, 2023.

HIJMANS, R. J. et al. **Package 'terra'**. 2023. Available from: <https://cran.r-project.org/web/packages/terra/terra.pdf>. Visited on: 4 Nov. 2023.

HULIN, M.; CAILLAUD, D.; ANNESI-MAESANO, I. Indoor air pollution and childhood asthma: variations between urban and rural areas. **Indoor Air**, Wiley Online Library, v. 20, n. 6, p. 502–514, 2010. DOI: 10.1111/j.1600-0668.2010.00673.x.

JULIÁN, C. I. F.; ES, U.; FERRI, C. Airvlc: An application for real-time forecasting urban air pollution. In: CITESEER. PROCEEDINGS of the 2nd international workshop on mining urban data, Lille, France. [S.l.: s.n.], 2015. v. 11.

KAZEMI GARAJEH, M. et al. Monitoring trends of CO, NO2, SO2, and O3 pollutants using time-series sentinel-5 images based on google earth engine. **Pollutants**, MDPI, v. 3, n. 2, p. 255–279, 2023. DOI: 10.3390/pollutants3020019.

KURIYAMA, G. S.; MOREIRA, J. C.; SILVA, C. R. S. d. Exposição ocupacional ao dióxido de nitrogênio (NO2) em policiais de trânsito na cidade do Rio de Janeiro. **Cadernos de Saúde Pública**, SciELO Public Health, v. 13, p. 677–683, 1997.

LEE, H. J.; CHATFIELD, R. B.; BELL, M. L. Spatial analysis of concentrations of multiple air pollutants using NASA DISCOVER-AQ aircraft measurements: Implications for exposure assessment. **Environmental Research**, Elsevier, v. 160, p. 487–498, 2018. DOI: 10.1016/j.envres.2017.10.017.

LEE, H. J.; LIU, Y.; CHATFIELD, R. B. Neighborhood-scale ambient NO2 concentrations using TROPOMI NO2 data: Applications for spatially comprehensive exposure assessment. **Science of The Total Environment**, Elsevier, v. 857, p. 159342, 2023. DOI: 10.1016/j.scitotenv.2022.159342.

MENEZES, G. Uma rápida introdução ao geobr (R). **ResearchGate, s/n, Pelotas**, 2023.

MENG, Z.-Y. et al. Ambient sulfur dioxide, nitrogen dioxide, and ammonia at ten background and rural sites in China during 2007–2008. **Atmospheric Environment**, Elsevier, v. 44, n. 21-22, p. 2625–2631, 2010. DOI: 10.1016/j.atmosenv.2010.04.008.

MIRANDA, R. M. de et al. Urban air pollution: a representative survey of PM 2.5 mass concentrations in six Brazilian cities. **Air Quality, Atmosphere & Health**, Springer, v. 5, p. 63–77, 2012. DOI: 10.1007/s11869-010-0124-1.

PEBESMA, E. Simple Features for R: Standardized Support for Spatial Vector Data. **The R Journal**, v. 10, n. 1, p. 439–446, 2018. DOI: 10.32614/RJ-2018-009. Available from: <https://doi.org/10.32614/RJ-2018-009>.

RANA, A. D. et al. Modeling of tropospheric NO2 column over different climatic zones and land use/land cover types in South Asia. **Journal of Atmospheric and Solar-Terrestrial Physics**, Elsevier, v. 168, p. 80–99, 2018. DOI: 10.1016/j.jastp.2018.01.022.

SAFIEDDINE, S. et al. Tropospheric ozone and nitrogen dioxide measurements in urban and rural regions as seen by IASI and GOME-2. **Journal of Geophysical Research: Atmospheres**, Wiley Online Library, v. 118, n. 18, p. 10–555, 2013. DOI: 10.1002/jgrd.50669.

SHAMI, S. et al. Trends of CO and NO2 Pollutants in Iran during COVID-19 pandemic using Timeseries Sentinel-5 images in Google Earth Engine. **Pollutants**, MDPI, v. 2, n. 2, p. 156–171, 2022. DOI: 10.3390/pollutants2020012.

SHEEL, V. et al. Comparison of satellite observed tropospheric NO2 over India with model simulations. **Atmospheric Environment**, Elsevier, v. 44, n. 27, p. 3314–3321, 2010. DOI: 10.1016/j.atmosenv.2010.05.043.

SILVA, C. M. d. S. A expansão agrícola e suas relações com as concentrações atmosféricas do nitrogênio reativo sobre o cerrado brasileiro, 2023.

SOUZA, A. de et al. Spatio-temporal variations of tropospheric nitrogen dioxide in South Mato Grosso based on remote sensing by satellite. **Meteorology and Atmospheric Physics**, Springer, v. 134, n. 1, p. 19, 2022. DOI: 10.1007/s00703-021-00855-5.

SOUZA, E. G. d. et al. Análise espacial e temporal da concentração de dióxido de nitrogênio (NO2) no Brasil (2017-2021): impactos das medidas de restrição da pandemia de COVID-19 na redução da poluição atmosférica. **Boletim Geográfico do Rio Grande do Sul**, n. 39, p. 59–77, 2022.

SOUZA, R. C.; AZEVEDO, M. S.; DELLA JUSTINA, E. Monitoramento Ambiental do dióxido de Nitrogênio

(NO2) na Área Urbana de Porto Velho–RO utilizando Amostradores Passivos. **Geografia (Londrina)**, v. 30, n. 1, p. 387–404, 2021. DOI: 10.5433/2447-1747.2021v30n1p387.

SU, J. G. et al. An innovative land use regression model incorporating meteorology for exposure analysis. **Science of the total environment**, Elsevier, v. 390, n. 2-3, p. 520–529, 2008. DOI: 10.1016/j.scitotenv.2007.10.032.

TABUNSCHIK, V.; GORBUNOV, R.; GORBUNOVA, T. Unveiling air pollution in crimean mountain rivers: analysis of sentinel-5 satellite images using google earth engine (GEE). **Remote Sensing**, MDPI, v. 15, n. 13, p. 3364, 2023. DOI: 10.3390/rs15133364.

VALADÃO, L. V. et al. Avaliação dos Efeitos do Isolamento Social nos Níveis de NO2, Durante a Pandemia de COVID-19, em Áreas Urbanas de Brasília, Anápolis e Goiânia, por Meio de Sensoriamento Remoto. **Rev. Bras. Cartogr**, v. 74, n. 3, 2022. DOI: 10.14393/rbcv74n3-65537.

VEEFKIND, J. P. et al. TROPOMI on the ESA Sentinel-5 Precursor: A GMES mission for global observations of the atmospheric composition for climate, air quality and ozone layer applications. **Remote Sensing of Environment**, Elsevier, v. 120, p. 70–83, 2012. DOI: 10.1016/j.rse.2011.09.027.

VÎRGHILEANU, M. et al. Nitrogen Dioxide (NO2) Pollution Monitoring with Sentinel-5P Satellite Imagery over Europe during the Coronavirus Pandemic Outbreak. **Remote Sensing**, MDPI, v. 12, n. 21, p. 3575, 2020. DOI: 10.3390/rs12213575.

WICKHAM, H. The Split-Apply-Combine Strategy for Data Analysis. **Journal of Statistical Software**, v. 40, n. 1, p. 1–29, 2011. Available from: <https://www.jstatsoft.org/v40/i01/>.

WICKHAM, H. **ggplot2: Elegant Graphics for Data Analysis**. [S.l.]: Springer-Verlag New York, 2016. ISBN 978-3-319-24277-4. Available from: <https://ggplot2.tidyverse.org>.

WICKHAM, H.; HESTER, J.; BRYAN, J. **readr: Read Rectangular Text Data**. 2024. Available from: <https://readr.tidyverse.org>.

XIE, Y. **Dynamic Documents with R and knitr**. 2nd. Boca Raton, Florida: Chapman and Hall/CRC, 2015. ISBN 978-1498716963. Available from: <https://yihui.org/knitr/>.

ZHAO, X. et al. Assessment of the quality of TROPOMI high-spatial-resolution NO2 data products in the Greater Toronto Area. **Atmospheric Measurement Techniques**, Copernicus Publications Göttingen, Germany, v. 13, n. 4, p. 2131–2159, 2020. DOI: 10.5194/amt-13-2131-2020.